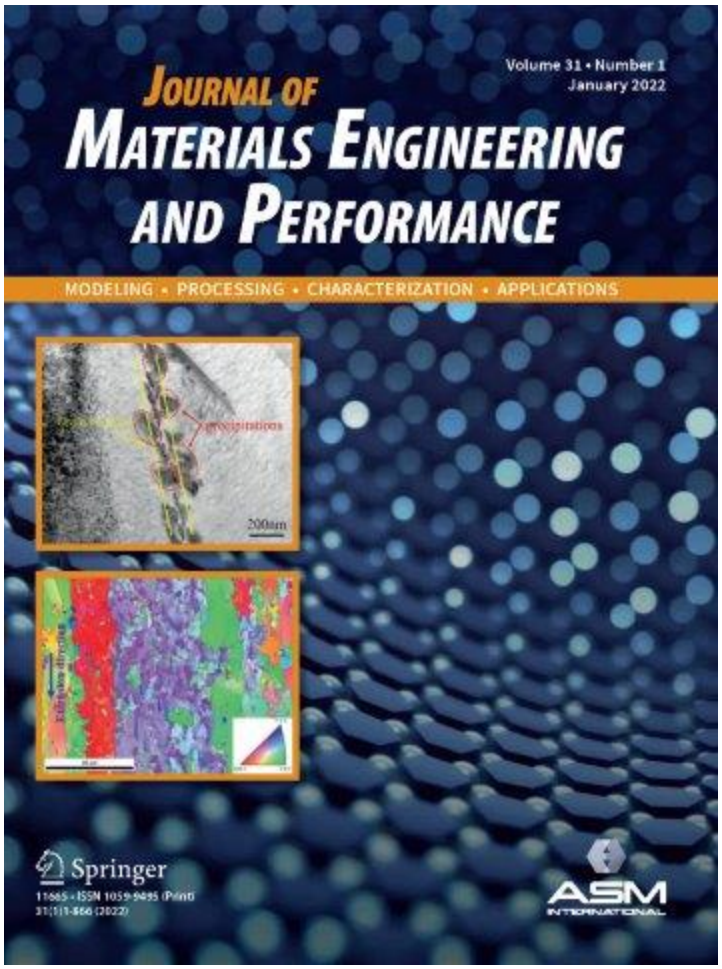

EFFECT OF HEATING RATE ON MARTENSITE TO AUSTENITE TRANSFORMATION KINETICS IN SUPERMARTENSITIC STAINLESS STEEL WELD DEPOSIT

Journal:	*Journal of Materials Engineering and Performance*
Manuscript ID	JMEP-21-09-25562.R2
Manuscript Type:	Technical Article
Date Submitted by the Author:	n/a
Complete List of Authors:	Zappa, Sebastian; Universidad Nacional de Lomas de Zamora; Consejo Nacional de Investigaciones Científicas y Técnicas Hoyos, John; Universidad de Buenos Aires, Departamento de Ingeniería Mecánica Tuffaro, Leonardo; Universidad de Buenos Aires, Departamento de Ingeniería Mecánica; Instituto Nacional de Tecnología Industrial Svóboda, Hernán; Consejo Nacional de Investigaciones Científicas y Técnicas; Universidad de Buenos Aires, Departamento de Ingeniería Mecánica

Keywords:	Dilatometry, Lever Ruler, Post-Welding Heat Treatments, Critical Temperatures, Transformation Rate

EFFECT OF HEATING RATE ON MARTENSITE TO AUSTENITE TRANSFORMATION KINETICS IN SUPERMARTENSITIC STAINLESS STEEL WELD DEPOSIT

Sebastián Zappa[1,2] (zappasebastian@hotmail.com), John J. Hoyos[3] (johnhosquin@gmail.com), Leonardo N. Tufaro[3,4] (ltufaro@inti.gob.ar), Hernán G. Svoboda[2,3] (hsvobod@fi.uba.ar)

[1] Universidad Nacional de Lomas de Zamora, Facultad de Ingeniería, Buenos Aires, Argentina.
[2] Consejo Nacional de Investigaciones Científicas y Técnicas, Buenos Aires, Argentina.
[3] Universidad de Buenos Aires, Facultad de Ingeniería, Departamento de Ingeniería Mecánica, Buenos Aires, Argentina.
[4] Instituto Nacional de Tecnología Industrial, Buenos Aires, Argentina

ABSTRACT

The supermartensitic stainless steels (SMSS) have a better combination of weldability, toughness and corrosion resistance than conventional martensitic and duplex stainless steels. Nevertheless, for both base material and weld deposit, heat treatments (inter and sub critical tempering) are required to control the resultant microstructure. A tempered martensite microstructure with a high content of reformed austenite, obtained after a post-weld heat treatment, improves the properties of SMSS weld deposits. The comprehension of austenite formation during post-weld heat treatment in weld metal deposits is a key aspect to predict the final properties. In the present work, the transformation kinetics of martensite into austenite in SMSS all-weld metal deposit was studied by dilatometry, considering the effect of the heating rate (1, 10, and 100 °C/s). In addition, the austenitic transformation kinetic was modeled by a sigmoidal equation. The increase of the heating rate increases Ac1 and Ac3, and reduces the range of the transformation (Ac3 – Ac1) from 120 to 80 ºC. The maximum transformation rate reached values of 0.023, 0.018, and 0.019 1/°C for 1, 10, and 100 °C/s, respectively. Thus, the maximum transformation rate was reached for the slowest heating rate. Nevertheless, the average transformation rate increased as a function of the heating rate. This could be associated with a change in the transformation mechanism.

Keywords: Dilatometry; Lever Ruler; Post-Welding Heat Treatments; Critical Temperatures; Transformation Rate

1. INTRODUCTION

Supermartensitic stainless steels (SMSS) are Fe-based alloys with very low C content (0.01 wt%), 11-13 % of Cr, 1.5-6 wt% of Ni and 0-2.5 wt% of Mo, with a microstructure predominantly martensitic [1]. In recent years, SMSS have been widely used with in oil and gas applications replacing classic martensitic and duplex stainless steels, because of the enhanced combination of weldability, toughness, and corrosion resistance and the ease of performing heat treatments, at a comparatively lower price [2-4]. In this sense, these materials are an economical alternative against uncoated carbon steels, carbon steel used without inhibitors or duplex stainless steels in some environments [5]. Furthermore, their relatively lower cost makes them an attractive option as a substitute for more expensive duplex and superduplex stainless steels, and their use in offshore deep water tubing applications has significantly increased in the last years [6].

Different heat treatments are usually used to adjust the microstructure and, therefore, the final properties. With a heat treatment at an inter-critical temperature (between Ac1 and Ac3, being Ac1 and Ac3 the initial and final transformation temperature of martensite into austenite during heating), it is possible to produce the tempering of the martensite, associated to the carbide precipitation, but also a certain content of a fine austenite at the martensitic lath boundaries is achieved. In this sense, during heating a certain amount of martensite transforms to austenite (this austenite is called reverted austenite) and can be stabilized upon cooling down to room temperature. The austenite metastable at low temperatures is called reformed austenite [7]. Under these conditions, the hardness decreases slightly, but the toughness increases significantly [8]. The stability of the reformed austenite particles is associated with elemental partitioning phenomena that are generated at the bi-phasic field ($\alpha + \gamma$) during heat treatment [9]. The lower the fraction of the equilibrium phase formed (i.e. γ), the greater the enrichment in the stabilizing elements (i. e. Ni) [9]. This enrichment is one of the mechanisms that stabilizes the reformed austenite. Furthermore, according to the literature [9], this austenite epitaxially grows from the inter-lath austenite films of a few atomic layers

in thickness. Reformed austenite holds a common orientation within a prior austenite grain (and its twins), strongly suggesting that reformed austenite inherits the original orientation of the austenite present prior to martensite formation. This effect is commonly referred to as the austenite memory effect. The transition from lamellar austenite in a two-phase microstructure to a classic one-phase austenite microstructure with few large grains with increasing time and temperature was reported to occur by steady spheroidization of lamellae, homogeneous nucleation of spherical grains and subsequent grain growth. In this sense, the substructure and laminar morphology of the reformed austenite provides another mechanism of additional mechanical stability to the reformed austenite [9].

Ni is known to play a crucial role in SMSS to stabilize austenite at room tempering (RT), due to its enrichment in Ni during heating in an inter-critical tempering cycle [10]. If tempering is carried out at temperatures slightly above Ac1, the enriched austenite will be metastable at RT. On the other hand, if the treatment is performed at temperatures well above Ac1, the austenite will lose chemical enrichment and, consequently, its stability. Thus, the martensitic transformation is easily induced owing to the decrease of thermal instability of austenite [8, 11].

Recent investigations on the kinetics of transformation of martensite into austenite in SMSS show that it takes place in two stages [12, 13]. Frank Niessen et al. [13] observed that the first stage involves the transformation of approximately 75% austenite, while the second stage involves the remaining 25%. The mechanism that determines the transformation rate of the first stages depends on the diffusion of Ni in martensite. However, the mechanism that determines the transformation rate of the second state depends on the diffusion of Ni in the austenite [13]. A change in HR led to a shift of the temperature of maximum transformation rate. In this sense, Bojack et al. [12], for dilatometry measurements, obtained similar results. The first stage of austenite formation is mainly due to partitioning of Ni and Mn. The second stage of austenite transformation is probably governed by an increased diffusivity of Ni and Mn at higher temperatures together with the decomposition of carbides and nitrides. As the HR increases, the critical transformation temperatures increase. Furthermore, with increasing HR, more austenite was formed during the first stage. The second stage of austenite formation became less pronounced and even disappeared at the highest HR. Ni-rich zones are transformed first to reverted austenite during heating, followed by Ni-depleted zones, whereby the Ni-rich regions transform to austenite first, due to their lower Ac1-temperature [10].

During welding, the solidification of the weld metal of SMSS takes place in the range 1480 to 1460°C. In this interval the delta ferrite nucleates and grows. In the subsequent cooling, austenite is formed on the grain boundary of delta ferrite between 1380 and 1180°C. The main austenite to martensite transformation occurs in the range from 230 to 190°C [1]. Due to the high cooling rates, delta ferrite could be retained at RT as well as a small fraction of retained austenite, in a martensitic matrix, resulting in high hardness and low toughness and ductility [14]. Also, microsegregation takes place in the weld metal, usually showing a cellular or cellular-dendritic substructure, which has associated strong variations in the local chemical composition [14, 15]. This microsegregation level is dependent on the welding conditions and could affect the phase transformations in subsequent operations.

It has been reported [16], in SMSS weld deposit, that when the austenitization is produced at temperatures between 40 and 50 ° C above the Ac1 temperature, the highest content of reformed austenite at RT is obtained after cooling. In this sense, it is important to specifically determine the critical transformation temperature of martensite into austenite during heating to define the tempering temperature, since a post-weld heat treatment (PWHT) at an inappropriate temperature could give rise to a hard and brittle microstructure. In this way, it is possible to achieve a microstructure consisting mainly of tempered martensite with high content of reformed austenite at RT.

Also, it must be considered the original microsegregation generating during welding which can also affect the formation of reverted austenite [17]. This aspect is not present when considering reverted austenite formation in SMSS wrought materials. In this sense, there were not found previous works that discuss it in SMSS weld metals. Several works have been carried out in this regard for wrought SMSS, but it is scarce the information available related to weld metals. Particularly, there were not found works in the literature that study the effect of the heating rate (HR) in austenite transformation for SMSS weld deposits.

For these reasons, the determination of the austenite transformation kinetics is a very important issue to predict and to understand the microstructural evolution during a PWHT in SMSS weld metal. In this sense, the HR is one of the variables of PWHT which affects the mentioned austenite transformation kinetics [1]. For some applications, like laser or induction heating are used to perform

an online PWHT, reaching higher heating rates that usually used [18, 19]. As mentioned above, the appropriate selection of the PWHT temperature is a determining factor to obtain the adequate microstructure that guarantees the desired properties.
The objective of this work was to study the transformation kinetics of martensite to austenite of a SMSS all-weld metal deposit by dilatometry, considering the effect of the HR (1, 10, and 100 °C/s).

2. EXPERIMENTAL PROCEDURE

2.1 Materials and welding

In order to meet the proposed objectives, an all-weld metal coupon was welded using a 13 % Cr SMSS tubular wire filler material of 1.2 mm diameter and carbon steel plates of 3/4" thick, according to the requirements of AWS A5.22 standard [20]. This type of test coupon is designed to evaluate the weld metal, independently of the base material. The characteristics of the weld metal are only related with the filler material and the welding conditions. The Metal Cored Arc Welding (MCAW) welding process was used, with Ar + 5% He gas protection and a flow rate of 18 l/min. The coupon was welded in a flat position, the electrode-piece distance was approximately 20 mm, and preheat and interpass temperatures were 100 °C. Table 1 shows the chemical composition of the consumable reported by the manufacturer [21]. Table 2 shows the welding parameters used. These parameters were determined based on previous works of the authors [2, 14, 16].

Table 1.- Chemical composition of the SMSS consumable [21]

Consumable	C	Mn	Si	Cr	Ni	Mo	N
	[ppm]	[%wt]	[%wt]	[%wt]	[%wt]	[%wt]	[ppm]
SMSS	<100	1.8	0.4	12.5	6.7	2.5	<100

Table 2.- Welding parameters used

Coupon	Tension	Current	Time	Length	Speed	Heat input
	[V]	[A]	[s]	[mm]	[mm/s]	[kJ/mm]
SMSS	29	298	92	460	5	1.7

2.2 Samples extraction

Specimens were extracted entirely from the all weld metal zone, as it is indicated in the figure 1. Their thickness was 2 mm. This zone is located in the center of the welded coupon and is free from dilution with the adjacent sheets. Hence, the weld deposit, and consequently the specimens have the chemical composition delivered by the filler material. To guarantee precision in machining, the electrical discharge machining (EDM) cutting technique was used with a 0.2 mm diameter molybdenum wire.

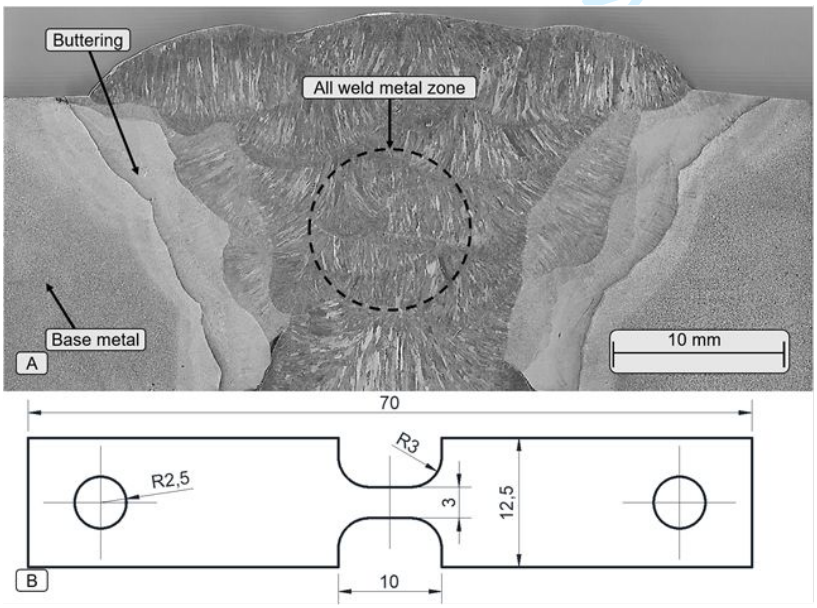

Figure 1.- A: All weld metal coupon for SMSS; B: Geometry of the specimens for dilatometry tests, units in mm

Figure 1.A shows the cross section of the welded coupon where different zones can be observed: base plates, buttered area and the central area of all weld metal zone, from where the samples were extracted for the dilatometry study. Figure 1.B shows the geometry of the dilatometry specimens used.

2.3 Microstructural characterization of the AWC

In order to characterize the initial microstructure, on the cross section, in the area of the all-weld metal zone, the chemical composition was determined by optical emission spectrometry (OES), except for the C, O, N and S contents that were analyzed by combustion technique. The samples were extracted by EDM. The microstructural characterization was performed by Scanning Electron Microscopy (SEM) and X-Ray Diffraction (XRD). Samples were mechanically polished and etched before SEM observation. Vilella's reagent (95 ml ethanol, 5 ml HCl, 1g picric acid) was used to reveal the microstructure. XRD test was carried out at the Thermo-Mechanical Simulation Experimental Station (XTMS) of the LNNano (Laboratório Nacional de Nanotecnologia). This facility is located at the XRD-1 beamline of the Brazilian Synchrotron Light Laboratory (LNLS). The laboratories belong to the National Center for Research in Energy and Materials (CNPEM, Campinas, Brazil). XRD was performed with synchrotron radiation (12 keV and λ = 0,10332 Å) within a scan range of 28 – 88° (2θ). The retained austenite contents were determined using the peak comparison method from the XRD patterns [22]. Ferrite content was measured by quantitative metallography following ASTM E562-02 standard [23].

2.4 Dilatometry

Dilatometry studies were carried out in order to determine the critical transformation temperatures (Ac1 and Ac3) of the weld metal. The HR is known to modify critical transformation temperatures. To study the aforementioned effect of the HR on the critical temperature shift, the studies were carried out in accordance with the parameters established in Table 3. These parameters were chosen from the literature review of the martensitic stainless steel, in order to compare the phase transformation kinetics of the SMSS weld deposit with that reported for the SMSS [10, 12, 13, 18, 19, 24].

Table 3.- Parameters of dilatometry studies

Coupon	Heating Rate [°C/s]	Temperature [°C]	Time hold [s]	Cooling rate [°C/s]
SMSS	1	1000	60	20
	10	1000	60	20
	100	1000	60	20

Figure 2 shows a diagram of the thermal cycles used. As in the XRD tests, dilatometry test was carried out at the XTMS of the LNNano. This Experimental Station has a unique and custom built thermo-mechanical simulator (GleebleTM 3S50). These tests were carried out under a vacuum atmosphere (10^{-1} Pa), with a type K thermocouple welded at the center of the calibrated length of the sample, and a laser dilatometer, which measures the change in cross section. For each case, dilatation, temperature and time were recorded during the applied thermal cycle, obtaining curves dilation vs temperature, from which Ac1, Ac3 and Ms temperatures were determined. Samples shown in Figure 1.B were used The measured length changes are higher than the dilatometer resolution (0.002 mm) and standard deviation (0.0016 mm).

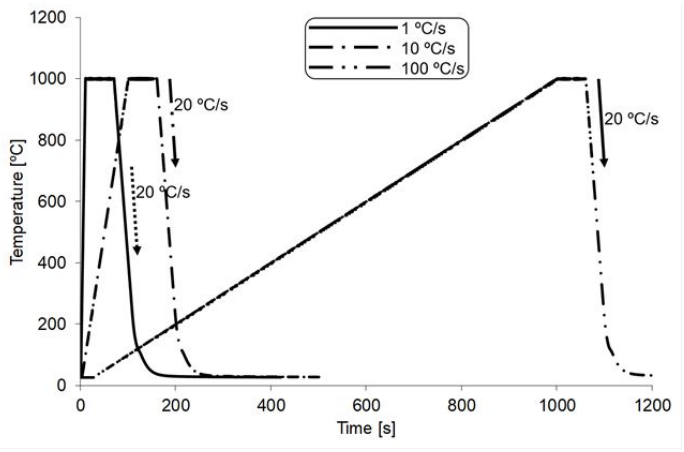

Figure 2.- Thermal cycles for different heating rates

To evaluate the austenite transformation during the heating in the dilatometry test [25], the lever rule was applied (Equation 1) as shown in Figure 3. In this figure it can be observed tree stages of the dilatation curve, corresponding to the linear expansion of the martensite during heating, the martensite to austenite transformation stage and the line of linear expansion of the austenite during heating. Using the lever rule to quantify phases implies assuming the following [26]: differences in specific phase volumes and relaxation of residual stresses are neglected; austenite and martensite are assumed to be the only phases present in the material; the expansion in the axis of dilation is assumed to be directly proportional to the total expansion of the volume.

$$A_{(T)} = (\Delta m_{(T)} - \Delta_{(T)})/(\Delta m_{(T)} - \Delta a_{(T)}) \quad \text{Equation 1}$$

Where $A_{(T)}$ is the austenite content for a specific temperature; $(\Delta m_{(T)} - \Delta_{(T)})$ is the specimen contraction for a temperature T; $(\Delta m_{(T)} - \Delta a_{(T)})$ is the total contraction.

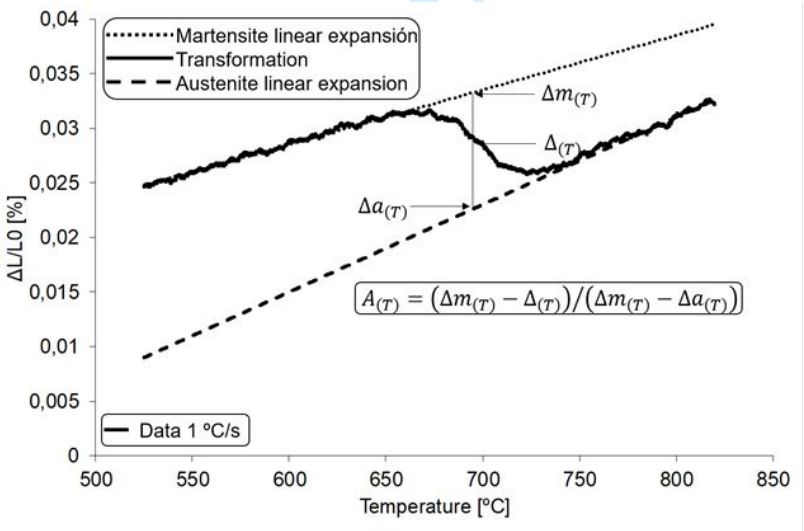

Figure 3.- Lever rule applied for the determination of austenite content

Finally, a comparison with different models reported in the literature, on the transformation of martensite into austenite, was carried out [27, 28]. Hence, the model proposed by Zotov et al. [29] was the one that best adjusted to the determined values. With this model, the kinetics of transformation of martensite into austenite during heating were studied. Thus, the kinetics of the austenitic transformation and its transformation rate were calculated using Equations 2 and 3, respectively.

$$A_{(T)} = 1/\left\{1 + e^{[-gv(T - T_m)]}\right\}^{1/v} \quad \text{Equation 2}$$

$$TR = dA_{(T)}/dT = gA_{(T)}\left(1 - (A_{(T)})^{v}\right) \quad \text{Equation 3}$$

Where the three fitting parameters g, v and T_m have simple physical meanings: T_m determines the temperature of the Maximum Transformation Rate (TR_{max}), g and v are related to the growth and nucleation rates, respectively.

3. RESULTS AND DISCUSSION

3.1 Weld metal characterization

Table 4 shows the chemical composition measured from the SMSS steel weld metal. The obtained values are according with the chemical composition of the filler metal reported by the manufacture, which was previously informed in the Table 1 [16]. The O and N content determined is in accordance with what is expected for this type of steel.

Table 4.- Chemical composition of the weld deposit

C	Mn	Si	S	P	Cr	Ni	Mo	Cu	V	Nb	O*	N*
[%wt]	[%wt]	[%wt]	[%wt]	[%wt]	[%wt]	[%wt]	[%wt]	[%wt]	[%wt]	[%wt]	[ppm]	[ppm]
0.012	1.76	0.44	0.013	0.015	12.13	6.27	2.69	0.49	0.09	0.01	390	50

In Figure 4 it can be seen a SEM image and XRD pattern of the $SMSS$ weld metal in AWC. Martensite with a low content of ferrite can be observed in the Figure 4.A [14]. Also, peaks corresponding to austenite and martensite/delta ferrite can be identify in the XRD pattern of the Figure 4.B. A predominantly martensitic matrix, with the presence of 9% delta ferrite (in its different morphologies) and 3% retained austenite was observed. The presence of ferrite and austenite is due to the incomplete transformation into austenite and martensite, respectively, in solid state during cooling. As mentioned above, the ferrite and retained austenite content, control the final properties with opposite effects. A higher content of ferrite and retained austenite decreases and increases, respectively, the toughness and ductility of the weld deposits [16].

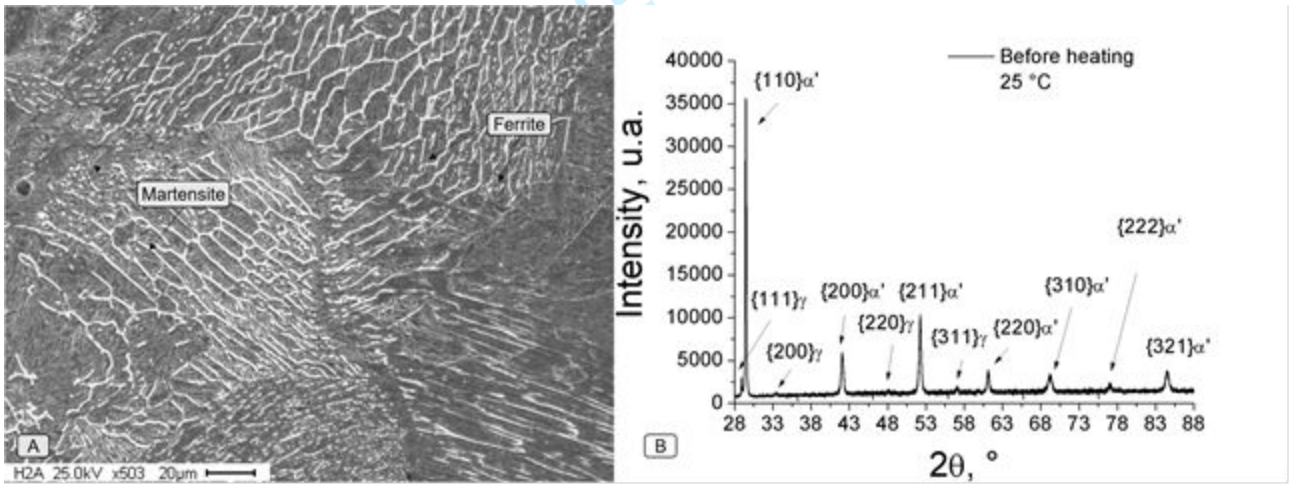

Figure 4.- Microstructure in as welded condition. A: SEM; B: XRD

3.2 Critical transformation temperatures

In martensitic stainless steel with high Ni content, Ac1 can be around 550 ºC [30]. In the literature there were proposed different equations to estimate Ac1, Equation 4, and Ms (initial critical temperature of transformation of austenite into martensite during the cooling), Equation 5 [16, 30, 31].

$$Ac1 = 850 - 1500(C + N) - 50Ni - 25Mn + 25Si + 25Mo + 20(Cr - 10) \quad \text{Equation 4}$$

$$Ms = 540 - 497C - 6.3Mn - 36.3Ni - 10Cr - 46.6Mo \quad \text{Equation 5}$$

The Ac1 and the Ms temperatures, calculated according to Equation 4 and 5 were 588 ºC and 49 ºC, respectively, for the SMSS weld deposit analyzed in this work. However, these equations are for reference only, since they do not consider heating rate, cooling rate, initial microstructure, segregations, etc.

3.3 Dilatometry

Figure 5 shows the dilatometry curves for different heating rate studies, A: 1 ºC/s, B: 10 ºC/s and C: 100 ºC/s, measured and filtered data. In these curves, the obtained initial and final critical temperatures of transformation of martensite into austenite, Ac1 and Ac3, during heating can be identified. Furthermore, Ms can also be observed. In this sense, the Mf (final critical temperature of transformation of austenite into martensite) could not be identified graphically, because it is under room temperature. Table 5 shows the values of critical temperatures experimentally determined.

Table 5.- Critical temperatures determined by dilatometry

Heating Rate [°C/s]	Ac1 [°C]	Ac3 [°C]	Ac3 – Ac1 [°C]	Ms [°C]
1	625	745	120	135
10	690	790	100	135
100	725	805	80	140

The initial and final critical temperature of transformation of martensite into austenite showed dependence with the heating rate in the analyzed welded deposit, as it was previously reported for other materials [13]. As the heating rate increased from 1 to 100 ºC/s, the Ac1 temperature increased. The same behavior was found for the Ac3 temperature, but more attenuated. The range of transformation of martensite into austenite (Ac3 – Ac1) decreases as the HR increases. These results show the importance of controlling the HR during the application of heat treatments, especially in those materials that have a narrow range of critical temperatures, such as SMSS [1, 30]. Figure 6 shows the variation of the critical transformation temperatures with the HR for the analyzed SMSS all-weld metal. The experimentally determined values were fitted with a potential equation, relating Ac1 and Ac3 with the HR, with a suitable R^2, Equation 6 and 7.

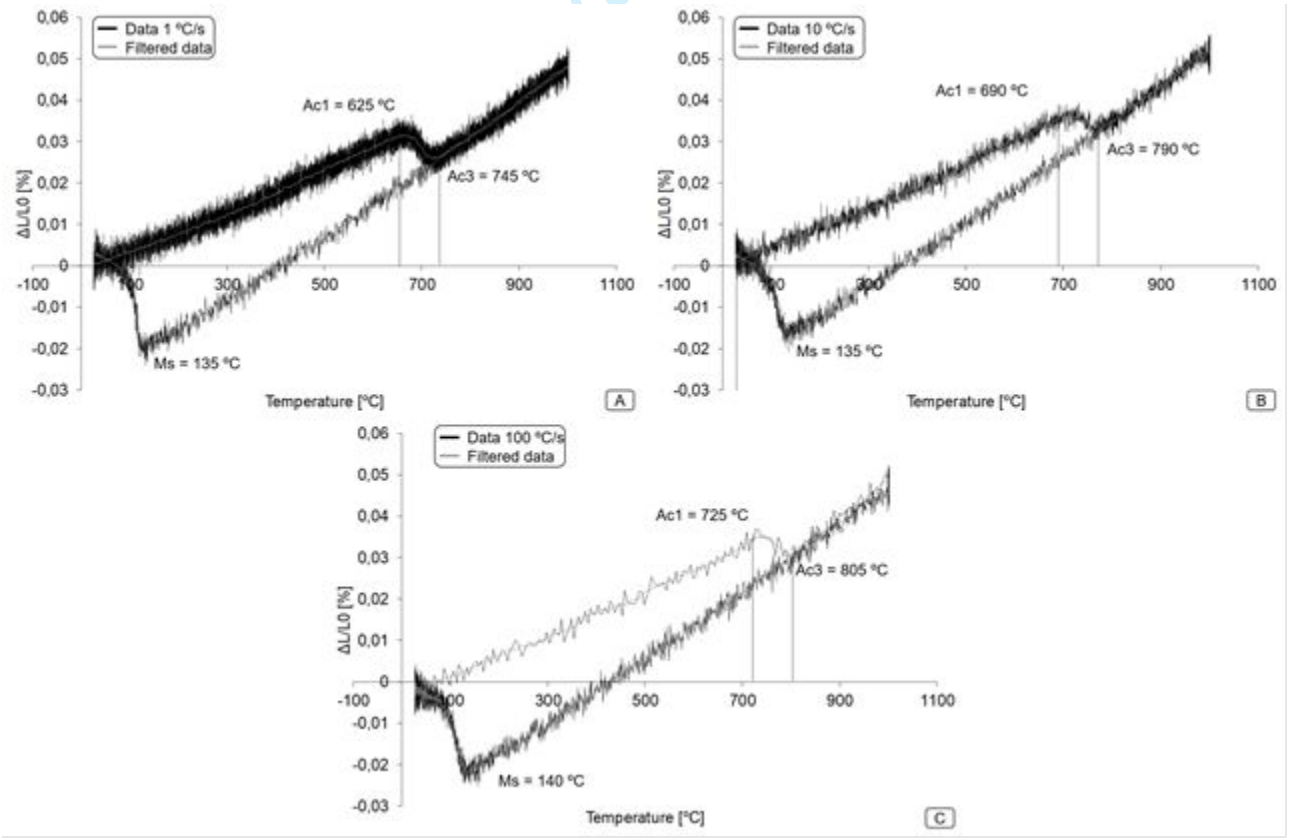

Figure 5.- Dilatometry curves for different heating rates: A- 1 °C/sec, B- 10 °C/sec, C- 100°C/sec. Filtered and real data.

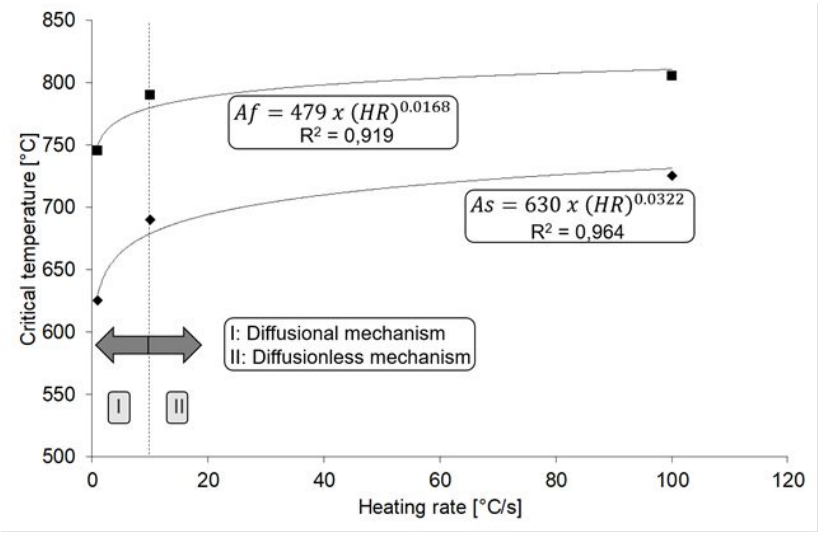

Figure 6.- Critical temperatures for different HR

$$Ac1 = 479\ x\ (HR)^{0.0168}$$ Equation 6

$$Ac3 = 630\ x\ (HR)^{0.0322}$$ Equation 7

It is noteworthy that the critical temperatures Ac1 and Ac3 increase with HR, showing a higher increase between 0 and 10°C/s. According to the literature [24], this behavior shows the change in the transformation mechanism of martensite into austenite with a limit of 10°C/s, above that threshold the transformation is generated by a non-diffusional mechanism. For high HR (above 10 ºC/s) there is not enough time to activate the diffusion and therefore the transformation is generated by diffusionless mechanism. Both lead to an austenitic lattice, however the resulting microstructures are completely different [27].

3.4 Austenite formation during heating

Figure 7 shows the kinetics of the austenite formation during heating for 1, 10 and 100 ºC/s. In addition, in Figure 7.D, the fit curves of the experimental results using the Zotov model are presented.

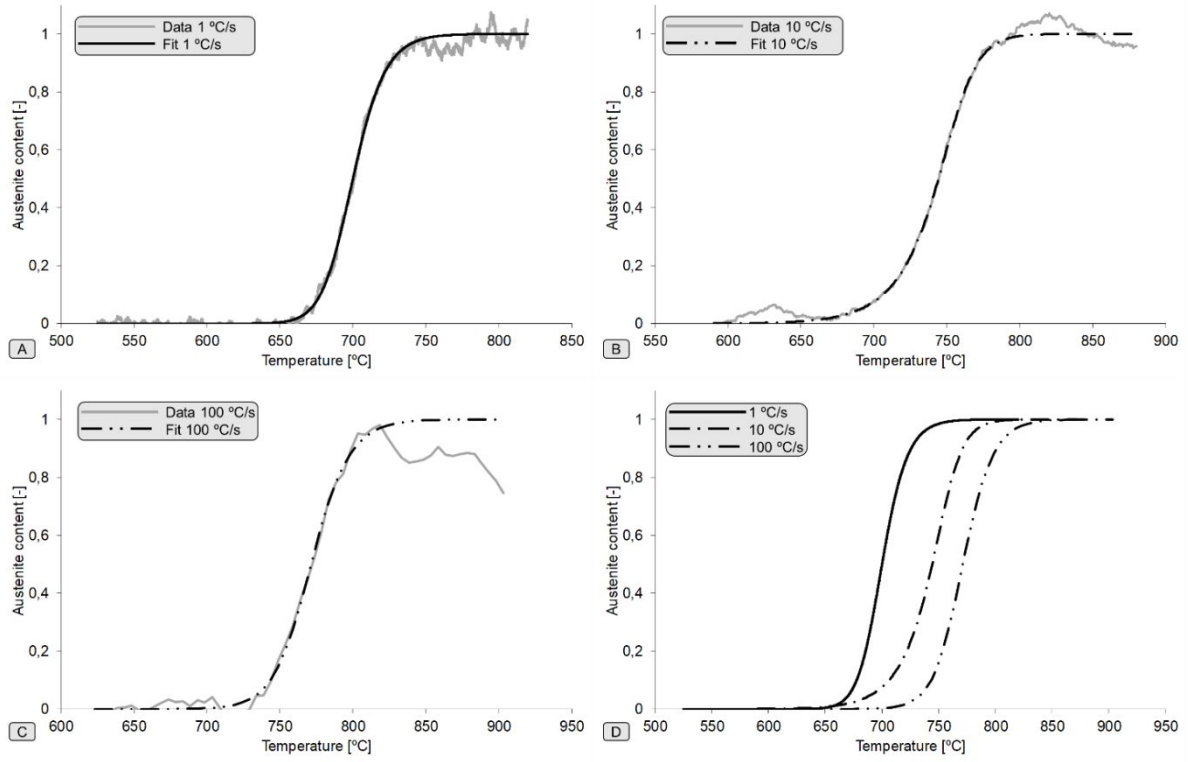

Figure 7.- A to C- Austenite transformation with temperature for different HR, determined from the dilatometry data. D- Comparison of obtained fitting curves

Bojack [10, 12] and Niessen [9, 13, 26] found that the transformation of martensite to austenite occurs in two stages. These authors observed a double state transformation at low heating rates (up to 10 K/min), in super martensitic stainless steels with a lower alloy content, in normalized condition. However, this two-stage kinetic behavior was not observed in the present work. The situation that explains the differences between the reported by the authors and the ones obtained in the present work could be associated with the differences in the heating rate, the chemical composition of the SMSS used and the microsegregation associated to the weld microstructure. In this sense, in a homogeneous microstructure there are few Ni-enriched zones that could act as austenite nucleation sites during heating. In these instances, in a first stage transformation, the reverted austenite that forms depends on Ni diffusion in the martensite (approximately 75% reverted austenite). This stage culminates when the Ni content of the adjacent zone to the austenite is consumed. In a second stage transformation (the last 25% of reverted austenite), the reverted austenite to be formed depends on Ni diffusion in the austenite. However, in as welded condition, the segregation level of the microstructure is very high and could affect the two stages transformation. Such segregation generates a greater number of enriched zones in gamma-forming elements that act as preferential sites for the nucleation of reverted austenite. In these instances, the transformation rate depends only on Ni diffusion in the residual martensite. This could be another of the reasons that explains the one stage transformation found in this article. Further studies are necessary to clarify this issue in supermartensitic stainless steel weld deposits.

The kinetics of transformation from martensite to austenite was also modeled by several phenomenological equations such as Exponential and Linear [29]. Both Exponential and Linear models displayed huge discrepancies with the experimental data. The first one considers a nucleation rate proportional to the volume fraction of martensite and the second one considers a constant nucleation rate. In addition, they both consider a zero-growth rate. In contrast, the alternative model proposed by Zotov et al. [29] allows a variable nucleation rate and a non-zero growth rate, which leads to a better fitting.

Figure 8 shows the transformation rate of martensite into austenite vs temperature and austenite content, for each heating rate. The values of the parameters g, v and T_m for the different heating rates are presented in the Table 6.

Table 6.- Parameters of Equations 2 and 3 $A_{(T)}$ and TR

Heating Rate	T_m	g	v
[°C/s]	[°C]	[°C]	[-]
1	693	0,123	0,657
10	757	0,045	2,127
100	768	0,084	0,850

The increase of the HR from 1 to 10 °C/s decreases the parameter g and increases the parameter v. This suggests a decrease in the growth rate of the austenite and an increase in the nucleation rate of the austenite. In contrast, the further increase of the heating rate until 100 °C/s does not follow the same trend. This could be related to the change in the transformation mechanism from diffusional to non-diffusional. For athermal phase transformations, the kinetic parameters could depend on temperature [29].

There is a relationship between v and the austenite content at the TR_{max}. If $v < 1$, the TR_{max} occurs below of 50% of austenite and if $v > 1$, it is for austenite contents higher than 50%, as it can be observed in the Figure 8.B. In all the analyzed cases, TR_{max} is close to 50% of austenite (0,45-0,59).

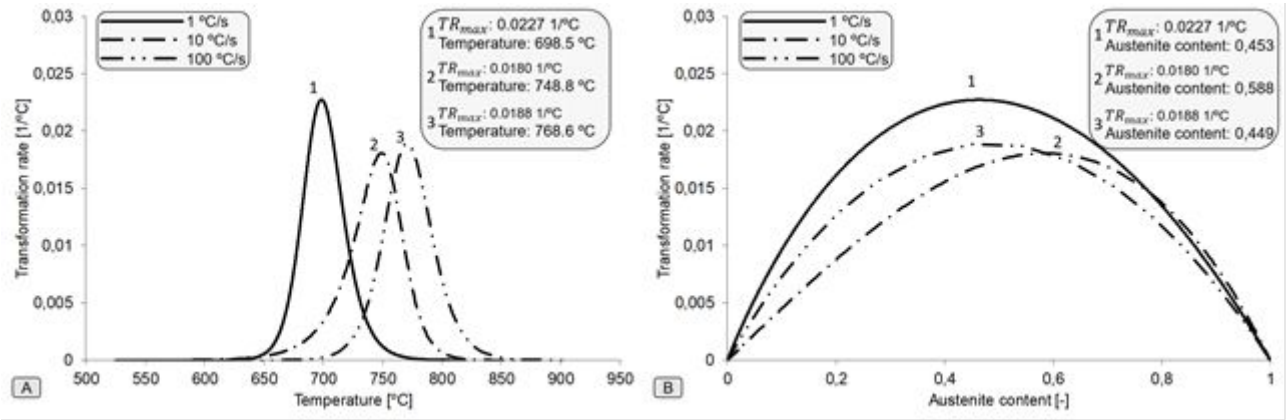

Figure 8.- Austenite formation kinetics. A: TR vs Temperature; B: TR vs Austenite

In this sense, according to what is observed in Figure 8, the transformation of martensite into austenite begins at the temperature Ac1, particular for each HR in a single stage. As can be seen in Figure 8.A, the initial TR is slow, due to the low temperature, and increases at higher temperatures. As the temperature increases, the TR increases, until reaching a TR_{max}. In this sense, a TR_{max} of 0.023, 0.018 and 0.019 1/ºC was observed for 1, 10 and 100 ºC/s, respectively. After this instance, as the temperature increases, the TR decreases. As can be seen in Figure 8.A and 8.B, the higher value of TR_{max} is reached with the lowest HR. As the HR increases the TR_{max} decreases. However, the Average Transformation Rate (TR_{Av}), represented by the area under the curves in Figure 8.A and 8.B, increases with increasing HR. This situation is clearly identified in Table 5, where it can be observed that as the HR increases from 1 to 100 ºC, the critical transformation range (Ac3 – Ac1) decreases from 120 to 80 ºC. Even, in addition to decreasing the range, it does so at a higher TR (the time required to complete the transformation is less).

As it was mentioned before, the role of Ni in stabilizing the austenite at RT in SMSS, could explain the observed results. Austenite is enriched in Ni during heating. Since Ni lowers the temperature Ac1, Ni rich zones are transformed first to austenite during heating, followed by Ni depleted zones [10] at low TR. The austenite content increases due to the segregation of gamma stabilizers elements and the TR is maximum at 50% austenite, approximately. The last part of austenite formation then takes place at higher temperatures due to the lower local Ni content.

The Ms (transformation temperature of austenite into martensite during cooling) for all conditions was 135-140 °C, remaining almost constant. At the same time, the literature [31] establishes a direct relationship between Ms and the retained austenite content in martensitic stainless steel. After the heat treatment, if the temperature Ms is low enough, there will be austenite retained at RT, since the Mf (final temperature of transformation of austenite into martensite during cooling), will be lower than the RT. Due to weld solidification structure, depleted zones in alloying elements such as C, Ni, Mn, Cr, and Mo could increase locally the Mf temperature, increasing the retained austenite content. Heat treatment of martensitic steels can induce carbide precipitation and decrease the C content of the matrix by raising the Ms. This effect will be less significant in alloys with low C content as SMSS [31]. On the other hand, the temperatures Ac1 and Ms obtained by Equations 4 and 5 were in both cases significantly lower than from the temperatures found experimentally. This highlights the limitation of the equations for estimating these critical temperatures for SMSS weld metal. The observed differences for Ac1 indicate that the real austenite formation initiates at higher temperatures than the predicted one, increasing the difference with HR, according to the expected tendency. In the case of Ms, as mentioned before, due to segregations the depleted zones could produce the observed increase in the transformation temperature.

4. CONCLUSIONS

The kinetics of martensite to austenite transformation was analyzed, considering the effect of heating rate between 1 and 100 °C/sec. It was found that the increase of the heating rate increases the critical transformation temperatures (Ac1 and Ac3). Experimental equations to describe this dependence were determined for both critical temperatures. In contrast, the transformation range (Ac3 – Ac1) decreased as the heating rate was increased. At 10 °C/s the kinetics of phase transformation changed. This was related to the change in the transformation mechanism of

martensite into austenite from diffusional to non-diffusional. As the heating rate increases, the maximum transformation rate decreased. Thus, the TR_{max} was 0.023, 0.018, and 0.019 1/°C at 1, 10, and 100 °C/s, respectively. Nevertheless, the average transformation rate increased with increasing the heating rate, reducing the range of the transformation from 120 to 80 °C. For all heating rates, the maximum transformation rate of martensite into austenite is between 40 and 60 % of reverted austenite. Similarly, the Ms was 135-140 °C for all conditions since the cooling rate was constant.

5. ACKNOWLEDGMENT

The authors wish to thank CONARCO-ESAB for the donation of the filler metals, Air Liquide for the donation of the shielding gases, LNLS (Laboratório Nacional de Luz Síncrotron) for the facilities of the tests, Leonardo Wu of LNNano (Laboratório Nacional de Nanotecnologia) for the assistance, at the FI-UNLZ, INTECIN and INTI for financial support.

6. REFERENCES

[1] J. C. Lippold and B. T. Alexandrov, Phase transformation during welding and postweld heat treatment of 12Cr-6,5Ni-2,5Mo supermartensitic stainless steel, Stainless Steel Word 2004, KCI Publishing BV, Netherlands, 2004, p 1-10, in English.
[2] S. Zappa, E. Surian and H. Svoboda, Effects of Welding Procedure on Corrosion Resistance and Hydrogen Embrittlement of Supermartensitic Stainless Steel Deposits, J. Iron Steel Res. Int., 2013, 20(12), p 124-132, in English.
[3] D. Zou, Y. Han, W. Zhang and X. Fang, Influence of Tempering Process on Mechanical Properties of 00Cr13Ni4Mo Supermartensitic Stainless Steel, J. Iron Steel Res. Int., 2010, 17(8), p 50-54, in English.
[4] D. Zou, Y. Han, D. Yan, D. Wang, W. Zhang and G. Fan, Hot workability of 00Cr13Ni5Mo2 supermartensitic stainless steel, Mater. Des., 2011, 32, p 4443-4448, in English.
[5] P. Bala Srinivasan, S.W. Sharkawy and W. Dietzel, Environmental Cracking Behavior of Submerged Arc-Welded Supermartensitic Stainless Steel Weldments, J. Mater. Eng. Perform., 2004, 13(2), p232-236, in English.
[6] G. Pieta, R. Leite, C. Kwietniewski, T. Clarke and T. Strohaecker, Evaluation of the Fracture Toughness of a SMSS Subjected to Common Heat Treatment Cycles in an Aggressive Environment, J. Mater. Eng. Perform., 2010, 19(9), p 1318 – 1324, in English.
[7] S. Godin, J. Hamel-Akré, D. Thibault, A. Serventi and P. Bocher, Ni and Mn enrichment effects on reformed austenite thermodynamical and low cycle fatigue stability of 13%Cr–4%Ni and 13%Cr–6%Ni stainless steels, 2020 Springer Nature 2(38): 1-12, in English.
[8] D. Zou, X. Liu, Y. Han, W. Zhang, J. Li and K. Wu, Influence of Heat Treatment Temperature on Microstructure and Property of 00 Cr 13 Ni 5 Mo 2 Supermartensitic Stainless Steel, J. Iron Steel Res. Int., 2014, 21(3), p 364-368, in English.
[9] F. Niessen, F. B. Grumsen, J. Hald and M. A. J. Somers, Formation and stabilization of reversed austenite in supermartensitic stainless steel, 24th International Federation for Heat Treatment and Surface Engineering Congress, Nice, France, 2017, in English.
[10] A. Bojack, L. Zhao, P. F. Morris and J. Sietsma, In-situ determination of austenite and martensite formation in 13Cr6Ni2Mo supermartensitic stainless steel, Mater. Charact., 2012, 71(5), p 77-86, in English.
[11] L. Yu-rong, Y. Dong, Y. Qi-long, S. Ji, Z. Kun-yu and J. Wen, Effect of Heat Treatment on Microstructure and Property of Cr13 Super Martensitic Stainless Steel, J. Iron Steel Res. Int., 2011, 18(11), p 60-66, in English.
[12] A. Bojack, L. Zhao, P. F. Morris and J. Sietsma, Austenite Formation from Martensite in a 13Cr6Ni2Mo Supermartensitic Stainless Steel, Metall. Mater. Trans. A, 2016, 47, p 1996-2009, in English.
[13] F. Niessen, M. Villa, J. Hald and M. A. J. Somers, Kinetics analysis of two-stage austenitization in supermartensitic stainless steel, Mater. Des., 2017(8), 116, p 8-15, in English.
[14] S. Zappa, H. Svoboda, M. Ramini, E. Surian and L. de Vedia, Improving Supermartensitic Stainless Steel Weld Metal Toughness, Weld. J., 2012, 91, p 83s-90s, in English.
[15] F. Niessen, N. Tiedje and J. Hald, Kinetics modeling of delta-ferrite formation and retainment during casting of supermartensitic stainless steel, Mater. Des., 2017, 118(15), p 138-145, in English.

[16] S. Zappa, H. Svoboda, E. Surian, Effect of Post-Weld Heat Treatment on the Mechanical Properties of Supermartensitic Stainless Steel Deposit, J. Mater. Eng. Perform., 2017, 26(2), p 514-521, in English.
[17] B. Rohit and N. R. Muktinutalapati, Austenite reversion in 18% Ni maraging steel and its weldments, Mater. Sci. Technol., p 1-8, in English.
[18] K. Hao, M. Gao, C. Zhang, R. Wu and X. Zeng, Achieving continuous cold rolling of martensitic stainless steel via online induction heat treatment, Mater. Sci. Eng., A, 2016, 739(2), p 1996-2009, in English.
[19] P. Krakhmalev, I. Yadroitsava, G. Fredriksson and I. Yadroitsev, In situ heat treatment in selective laser melted martensitic AISI 420 stainless steels, Mater. Des., 2015, 87(15), p 380–385, in English.
[20] "Specification for Stainless Steel Electrodes for Flux Cored Arc Welding and Stainless Steel Flux Cored Rods for Gas Tungsten Arc Welding", A5.22, AWS Standards, AWS, 1995.
[21] "Technical sheet ok tubrod 15-55", ESAB, 2004.
[22] B. D. Cullity and S. R. Stock, Elements of X Ray Diffraction, Prentice-Hall, 3rd Edition, 2001, p 351-354.
[23] "Standard Test Method for Determining Volume Fraction by Systematic Manual Point Count", E562, ASTM Standards, ASTM, 2002.
[24] D. S. Leem, Y. D. Lee, J. H. Jun, C. S. Choi, Amount of retained austenite at room temperature after reverse transformation of martensite to austenite in an Fe-13%Cr-7%Ni-3%Si martensitic stainless steel, Scripta Materiala 2001, 45, p 767-772, in English.
[25] Y. Lian, J. Huang, J. Zhang, C. Zhang, W. Gao and C. Zhao, Effect of 0.2 and 0.5% Ti on the microstructure and mechanical properties of 13Cr supermartensitic stainless steel, J. Mater. Eng. Perform., 2015, 24(11), p 4253 – 4259, in English.
[26] F. Nießen, M. Villa, D. Apel, O. Keßler, M. Reich, J. Hald and M. A. J. Somers, In Situ Techniques for the Investigation of the Kinetics of Austenitization of Supermartensitic Stainless Steel, Mater. Sci. Forum, 2017, 879, p 1381-1386, in English.
[27] H. Kooiker, E.S. Perdahcıoğlu and A.H. van den Boogaard, Combined athermal and isothermal martensite to austenite reversion kinetics, experiment and modelling, Mater. Des., 2020, 196, p 1-7. in English.
[28] M. Gómez, S. F. Medina and G. Caruana, Modelling of Phase Transformation Kinetics by Correction of Dilatometry Results for a Ferritic Nb-microalloyed Steel, ISIJ Int., 2003, 43(8), p 1228–1237, in English.
[29] N. Zotov, V. Marzynkevitsch and E. J. Mittemeijer, Evaluation of kinetic equations describing the martensite–austenite phase transformation in NiTi shape memory alloys, Journal of Alloys and Compounds, 2014, 616, p 385-393, in English.
[30] T. G. Gooch, P. Woollin and A. G. Haynes, Welding metallurgy of low carbon 13% chromium martensitic steel, Supermartensitic Stainless Steel ´99, Belgian Welding Institute, Belgian, 1999, 188-195, in English.
[31] W. Wu, L.Y. Hwu, D.Y. Lin and J.L. Lee, The Relationship Between Alloying Elements and Retained Austenite in Martensitic Stainless Steels Welds, Scripta Materiala, 2000, 42, p 1071-1076, in English.

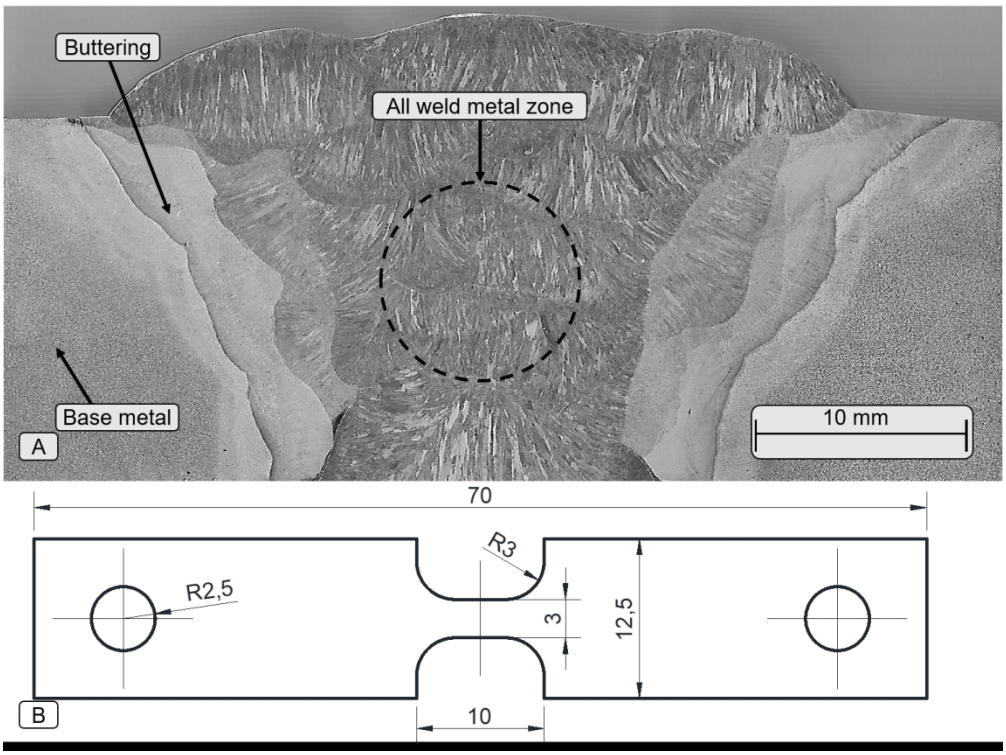

Figure 1.- A: All weld metal coupon for SMSS; B: Geometry of the specimens for dilatometry tests, units in mm

259x193mm (150 x 150 DPI)

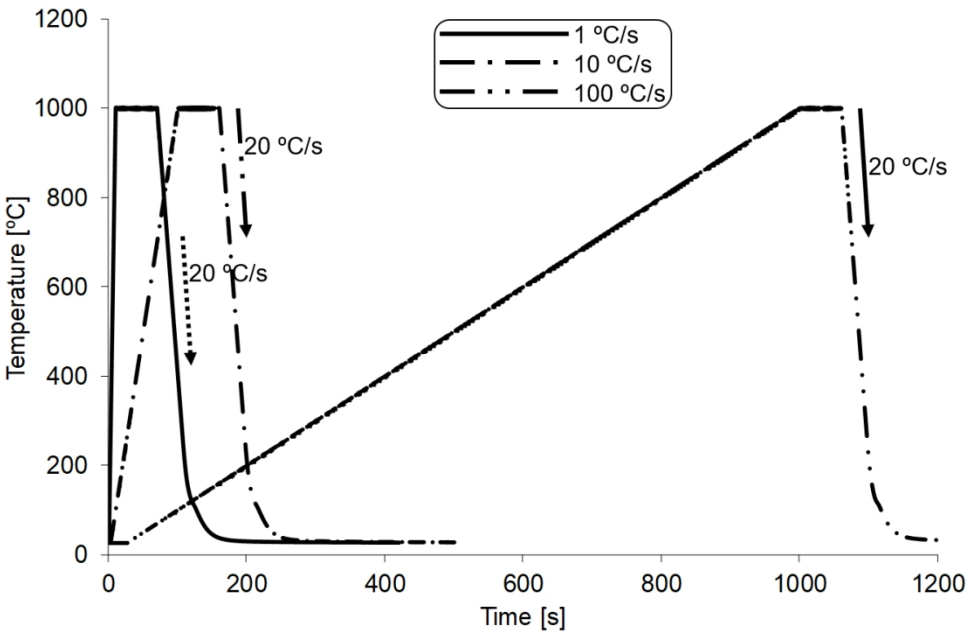

Figure 2.- Thermal cycles for different heating rates

231x150mm (150 x 150 DPI)

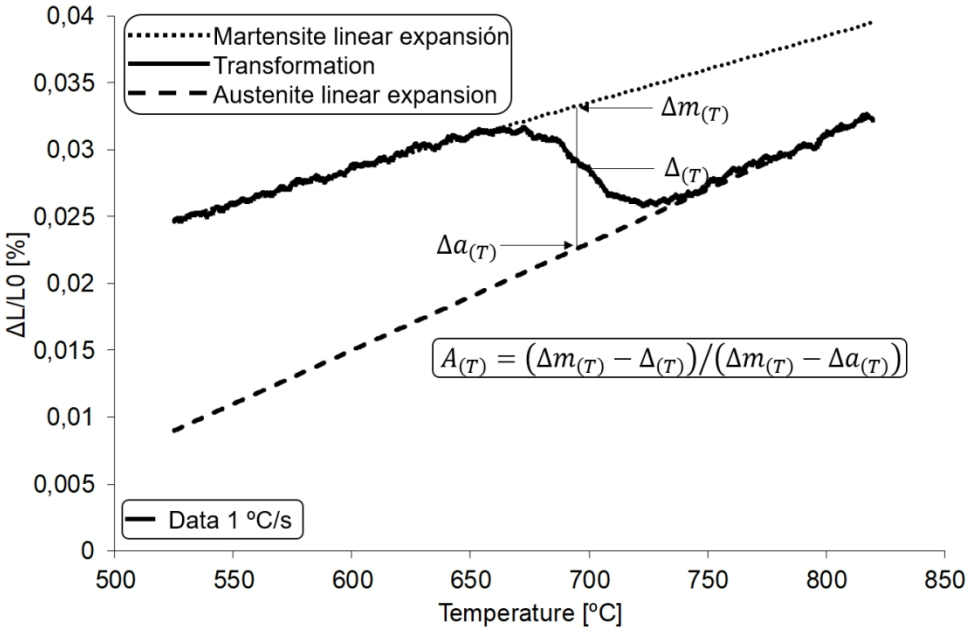

Figure 3.- Lever rule applied for the determination of austenite content

231x150mm (150 x 150 DPI)

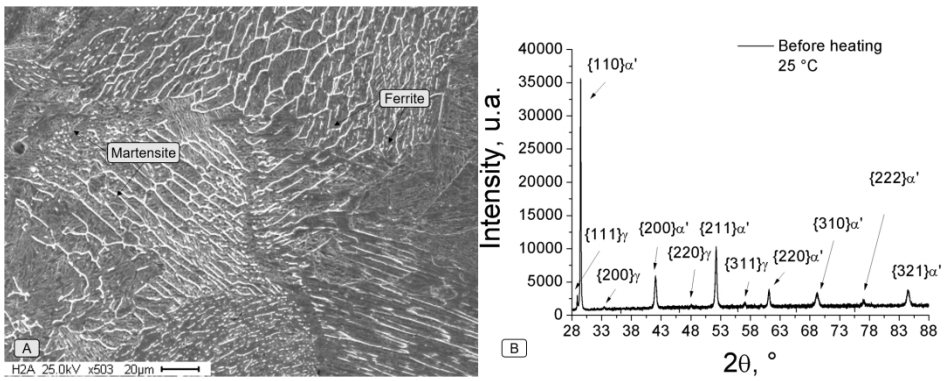

Figure 4.- Microstructure in as welded condition. A: SEM; B: XRD

404x150mm (150 x 150 DPI)

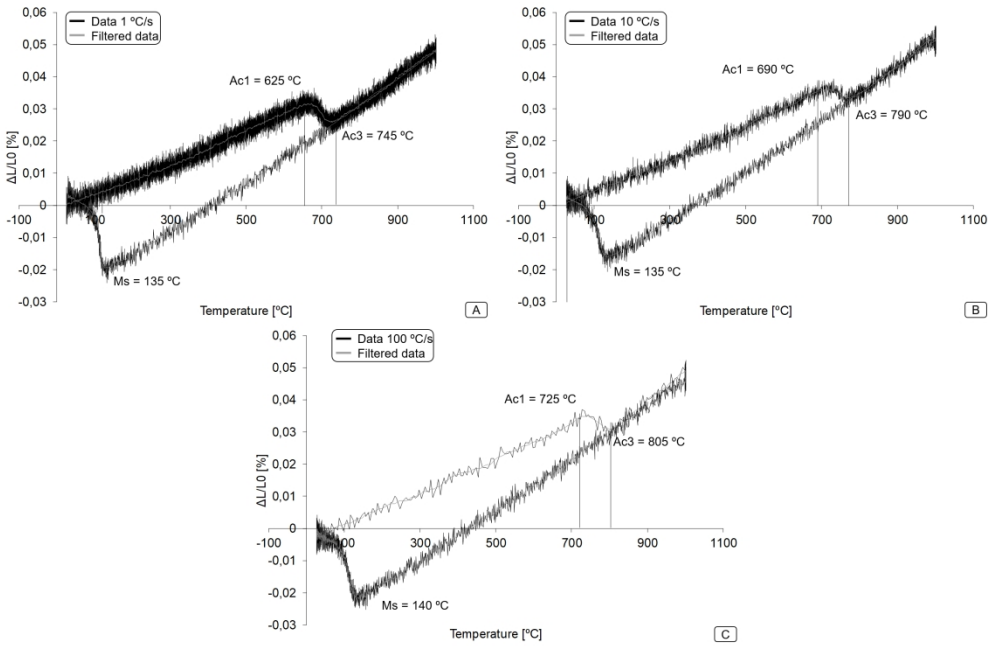

Figure 5.- Dilatometry curves for different heating rates: A- 1 °C/sec, B- 10 °C/sec, C- 100°C/sec. Filtered and real data.

463x300mm (150 x 150 DPI)

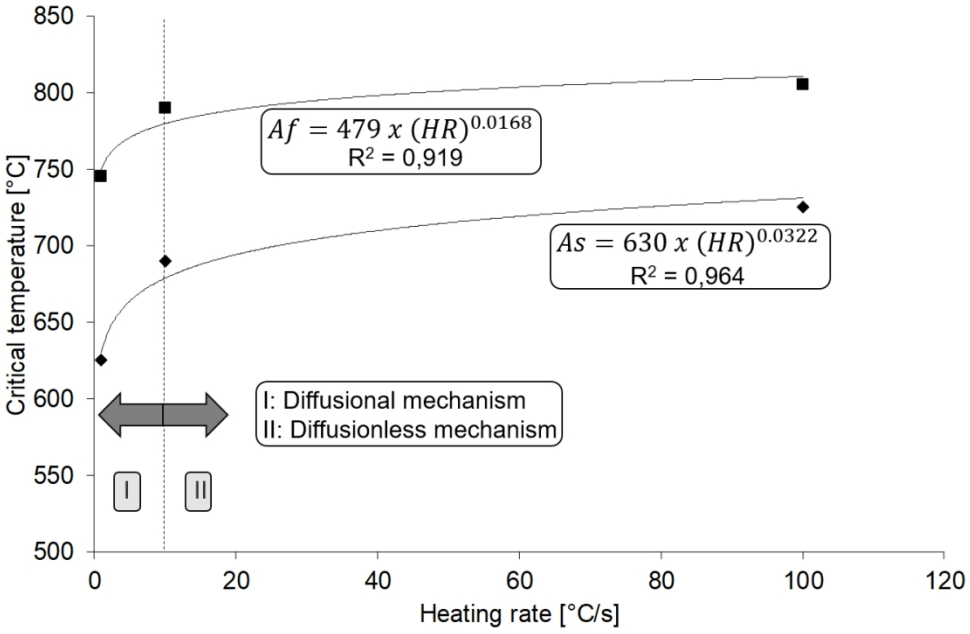

Figure 6.- Critical temperatures for different HR

231x150mm (150 x 150 DPI)

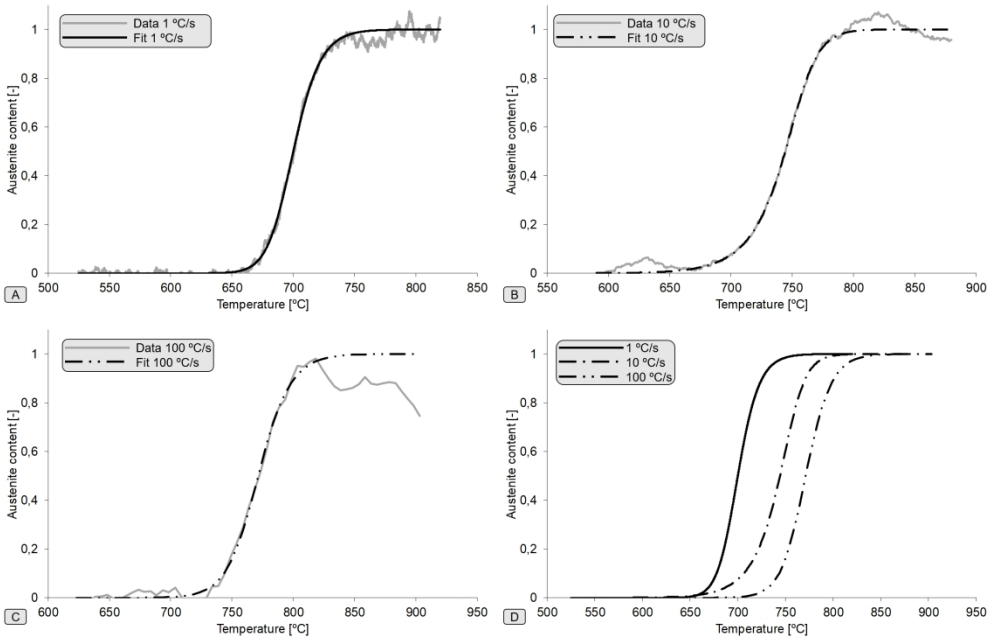

Figure 7.- A to C- Austenite transformation with temperature for different HR, determined from the dilatometry data. D- Comparison of obtained fitting curves

462x300mm (150 x 150 DPI)

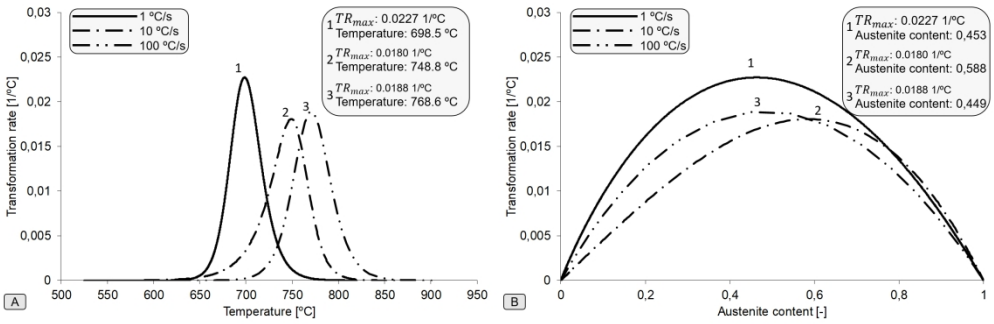

Figure 8.- Austenite formation kinetics. A: TR vs Temperature; B: TR vs Austenite

463x150mm (150 x 150 DPI)

Table 1.- Chemical composition of the SMSS consumable [19]

Consumable	C	Mn	Si	Cr	Ni	Mo	N
	[ppm]	[%wt]	[%wt]	[%wt]	[%wt]	[%wt]	[ppm]
SMSS	<100	1.8	0.4	12.5	6.7	2.5	<100

Table 2.- Welding parameters used

Coupon	Tension	Current	Time	Length	Speed	Heat input
	[V]	[A]	[s]	[mm]	[mm/s]	[kJ/mm]
SMSS	29	298	92	460	5	1.7

Table 3.- Parameters of dilatometry studies

Coupon	Heating Rate	Temperature	Time hold	Cooling rate
	[°C/s]	[°C]	[s]	[°C/s]
SMSS	1	1000	60	20
	10	1000	60	20
	100	1000	60	20

Table 4.- Chemical composition of the weld deposit

C	Mn	Si	S	P	Cr	Ni	Mo	Cu	V	Nb	O*	N*
[%wt]	[%wt]	[%wt]	[%wt]	[%wt]	[%wt]	[%wt]	[%wt]	[%wt]	[%wt]	[%wt]	[ppm]	[ppm]
0.012	1.76	0.44	0.013	0.015	12.13	6.27	2.69	0.49	0.09	0.01	390	50

Table 5.- Critical temperatures determined by dilatometry

Heating Rate	Ac1	Ac3	Ac3 – Ac1	Ms
[°C/s]	[°C]	[°C]	[°C]	[°C]
1	625	745	120	135
10	690	790	100	135
100	725	805	80	140

Table 6.- Parameters of Equations 6 and 7 $A_{(T)}$ and TR

Heating Rate	T_m	g	v
[°C/s]	[°C]	[°C]	[-]
1	693	0,123	0,657
10	757	0,045	2,127
100	768	0,084	0,850

JOURNAL OF
MATERIALS ENGINEERING
AND PERFORMANCE®

ASM INTERNATIONAL

PART A - COPYRIGHT TRANSFER

Manuscript Title: EFFECT OF HEATING RATE ON MARTENSITE TO AUSTENITE TRANSFORMATION KINETICS IN SUPERMARTENSITIC STAINLESS STEEL WELD DEPOSIT

Author(s): Sebastián Zappa, John J. Hoyos, Leonardo N. Tufaro, Hernán G. Svoboda

This transfer document must be signed by each author unless excepted below and be received by the Editorial Office before the article can be published. Other copyright transfer forms may not be substituted for this form, but this form may be photocopied for use. If the article is not published in the Journal of Materials Engineering and Performance, this copyright transfer will not take effect.

required: Has this manuscript been copyrighted, published, or submitted for publication elsewhere? Yes [ ] No [X]

(Note: Prior publication is a basis for rejection. However, appearance in a conference proceedings or similar special presentation with limited distribution is not necessarily prior publication. In such cases the article should be so referenced. If the box above is marked yes, the editorial office will contact you for details and then make a determination whether the journal will accept submission of this manuscript. If so, the authors must provide the appropriate reference information.)

Copyright, title, interest, and all rights, including subsidiary and/or derivative rights, in all languages in the article named above are hereby assigned and transferred to ASM International®, Materials Park, Ohio 44073-0002, effective when the article is accepted for publication in the Journal of Materials Engineering and Performance, subject to the rights below reserved by the author and/or employer.

ASM International shall have sole rights of distribution and publication of the work and its abstract in all forms and media, including the exclusive right to create electronic versions of the article, or by any other means, now known or later developed. The undersigned hereby represents and warrants that the work is original with him or her, that the work does not infringe any copyright, trademark, intellectual property rights, or other personal or proprietary rights in any other work, or violate any other rights of any third parties, and that he or she is the author of the work or is authorized to assign copyright of the work to ASM International by executing this agreement.

The author warrants that neither the work nor portions of it have been published elsewhere in any form, nor are being considered for publication elsewhere in any form. If this is not the case, ASM International must be notified and appropriate credits and permissions to republish must be attached. U.S. Government employees whose work is not subject to copyright may certify such employment status in Part B below.

The author retains the following:

1. All proprietary rights other than copyright, such as patent rights.
2. The right to make oral presentation or to personally reuse all or portions of the content of the work in other works of his own authorship, including lectures, textbooks, reviews, and articles, provided proper notice of ASM International's copyright is given.
3. The right to reproduce the work or parts thereof without revision or modification for the author's personal use, for lecture or educational purposes, to the extent the Fair Use Provisions of the U.S. Copyright Act permit, provided that all copies include proper notice of ASM International's copyright and indicate the source, and that no fees are collected for distribution or publication of the work. If the work was prepared by an employee within the scope of his or her employment, the employer shall have the right to make copies of the article for the employer's own internal use.

4. The right to post an electronic form of the final ASM International file of the work without revision or modification on the author's own personal or current employer's website, provided that such posting is noncommercial in nature and the work is made available to users without a fee or charge, and provided that proper notice of ASM's copyright is included. Such posting shall include a link to the journal homepage. The following statement must appear on the first page, or screen, of the work as posted:

   Copyright [year; for example, 2014] ASM International. This paper was published in [journal bibliographic information; for example, Journal of Materials Engineering and Performance, Vol. 23, Issue 1, pp. 99-108] and is made available as an electronic reprint with the permission of ASM International. One print or electronic copy may be made for personal use only. Systematic or multiple reproduction distribution to multiple locations via electronic or other means, duplications of any material in this paper for a fee or for commercial purposes, or modification of the content of this paper are prohibited.

5. The right to make limited distribution of the article or portions of the article.
6. The right to reproduce figures and extracts from the article with proper acknowledgment.

In the case of work performed under U.S. Government contract, ASM International® grants the U.S. Government royalty-free permission to reproduce all or portions of the article and to authorize others to do so for U.S. Government purposes.

required: Author's Signature: _____

required: Date: December 30, 2021

By signing my name above, I hereby certify that I am the person indicated and agree to all of the terms above.

If either case below applies to this manuscript, please check the appropriate box, download and send a copy to an authorized representative for their signature. An electronic signature is acceptable. After the form is complete, email a copy to vince.katona@asminternational.org.

required: Is this a case of "work made for hire?" yes [ ] no [X]

A "work made for hire" (a work prepared by an employee within the scope of his or her employment or commissioned as a work for hire by written agreement), an authorized representative of the employee should sign below.

_____

Signature and Position Print Name Date

PART B - U.S. GOVERNMENT EMPLOYEE CERTIFICATION

required: Are All authors of this manuscript employees of the U.S. Government? yes [ ] no [X]

I certify that all authors of the article are employees of the U.S. Government and performed this work as part of their employment: therefore, the article is not available for U.S. copyright protection.

_____

Authorized Signature Title

_____

Name of Government Organization Date